International Journal of Civil Engineering (2023) 21:603–615
https://doi.org/10.1007/s40999-022-00787-0

RESEARCH PAPER

The Effects of Drainage Conditions on the Cyclic Deformation Characteristics of Over Consolidated Clayey Soil

Guiping Nie[1] · Ying Liu[1] · Zhiyong Liu[2,3] · Zhixuan Liang[1] · Jianfeng Xue[2] · Yaowei Liang[1]

Received: 31 July 2022 / Revised: 27 October 2022 / Accepted: 16 November 2022 / Published online: 9 December 2022

Abstract
Drainage conditions and consolidation states can affect the deformation behaviour of clayey soil under cyclic loading. A series of cyclic triaxial tests were carried out on normally and over consolidated kaolin under both undrained (UD) and partially drained (PD) conditions. The effects of drainage conditions on the strain accumulation, excess pore water pressure (EPWP) and resilient modulus (Mr) of the soil are analysed under different over consolidation ratios and cyclic stress amplitudes. The results indicate that greater axial strain may accumulate under PD condition than under UD condition if the cyclic stress is small. With the increase of over consolidation ratio, lateral deformation in soils under PD condition is similar to those under UD condition. Meanwhile, a large axial strain could accumulate with a small amount accumulation in EPWP under UD condition or in volumetric strain under PD condition. The Mr of soil decreases as EPWP increases under UD condition or as volumetric strain increases under PD condition. For the over consolidated soil, Mr could degrade significantly with little accumulation in EPWP under UD condition or in volumetric strain under PD condition. For example, under an over consolidation ratio of 5 and UD condition, Mr degrades about 20–55% with EPWP accumulation of 2–13 kPa.

Keywords Cyclic triaxial test · Over consolidated soil · Deformation behaviour · Drainage conditions

1 Introduction

Clayey soil may encounter large deformation and stiffness degradation under cyclic loading [1–5]. The surcharge preloading method is widely used to reduce the deformation of clayey soil subjected to cyclic loading. After applying surcharge, the soil is over consolidated and its cyclic deformation behaviour would differ with over consolidated ratios (OCRs). During long-term cyclic loading, for example, traffic loading condition, EPWP generates and dissipates simultaneously, suggesting that partially drained (PD) condition should be considered when analysing the deformation of soils. Understanding the effects of drainage conditions on the cyclic deformation of over consolidated soil is critical in assessing the long-term settlement of geotechnical infrastructures under traffic loading.

To evaluate the long-term settlement of geotechnical infrastructures under traffic loading, cyclic tests are usually performed to study the deformation of soil [6–9]. The deformation behaviour of soil is affected by cyclic stress ratio, OCR, initial static deviatoric stress, mineral composition and the number of loading cycles [1–6, 8, 10, 11]. It has been found that the greater the OCR, the less the accumulated axial strain and EPWP [11].

The initial static deviatoric stress ratio (the ratio of the static deviatoric stress to effective confining pressure) affects the cyclic deformation of an over consolidated soft marine clay [8]. It has been found that there exists a critical initial static deviatoric stress ratio beyond that great strain accumulation and failure can be observed under cyclic loading.

The long-term undrained behaviour of a soft clay by some researchers [12]. The soil was consolidated to

✉ Zhiyong Liu
zhiyongliu@tongji.edu.cn; zy_liu110@163.com

[1] School of Civil Engineering and Architecture, Guangxi University, Nanning, Guangxi, China

[2] School of Engineering and Information Technology, University of New South Wales, Campbell, ACT, Australia

[3] Key Laboratory of Road and Traffic Engineering of Ministry of Education, Tongji University, Shanghai 201804, China

different OCRs and then cyclically loaded under an undrained (UD) condition in a triaxial cell. The authors found that due to the coupling effects of cyclic loading and creep, the EPWP in the over consolidated soil increases in the early loading stage and then reduces as the loading continues. A similar phenomenon was also reported on an over consolidated soft marine clay [13]. Cyclic torsional shearing tests were carried out on marine soft clay and it has been claimed that the stress–strain hysteresis curve is nearly linear in samples with high OCR values [13].

Among those studies, as the permeability of clay is low, cyclic tests were performed under undrained condition. There is limited study for the deformation behaviour of clay under different drainage conditions.

The effects of drainage condition on the deformation behaviour of soils subjected to cyclic loading have been studied in some research. The cyclic deformation behaviour of railway track foundation materials was tested under both undrained and free drainage conditions [14]. The instability of the material is associated with the generation of large EPWP under undrained conditions or associated with a rapid increase in volumetric strain accumulation in free drainage conditions [14]. For the cyclic behaviour of Wenzhou clay, it has been found that greater permeant strain accumulates in PD condition than in UD condition [15]. However, different effects of drainage conditions on the cyclic deformation of soils were reported by other researchers [16, 17]. The researchers tested the deformation behaviour of silty clay under different drainage conditions and observed greater strain accumulations in samples under UD condition [16, 17].

Based on the literature review, it has been found that (1) the effects of drainage conditions on the cyclic deformation behaviour of soils are not clear and need to be further investigated; (2) there are few studies on the deformation of over consolidated soil under different drainage conditions.

To investigate the effects of drainage conditions on the cyclic deformation of clayey soil with different consolidation states, cyclic triaxial tests were performed on kaolin. The strain accumulation, EPWP and stiffness of the soil are investigated under different OCRs, cyclic stress amplitudes and drainage conditions. The deformation mechanism of the soil is analysed based on the EPWP and volumetric strain accumulation under different drainage conditions.

2 Material and Test Program

An advanced Dynamic Triaxial Testing System at Guangxi University was used to perform the cyclic tests. The description of this system can be referred to the existing work [18].

The material used in this study was kaolin. The specific gravity is 2.6. The plastic limit and liquid limit are about 35% and 75%, respectively, with a plasticity index (PI) of about 40% [18]. As shown in Fig. 1a, the soil lies on the A-line in the Casagrande diagram. Figure 1b reveals the grain size distribution curve of the soil, which was determined using a laser particle size analyzer (Mastesizer 3000) made in Malvern Company, the United Kingdom. Considering the position of the kaolin in the Casagrande diagram and the grain size distribution curve, the used soil can be classified as highly compressible silt. The hydraulic conductivity is about 6×10^{-8} cm/s determined as per GB/T 50124-1999 [19]. Kaolin slurry with a water content of about 2 times of liquid limit was put into a Perspex tube and consolidated under a vertical pressure of 100 kPa to prepare samples. More details about the preparation of samples have been addressed in the existing work [18]. All samples had a diameter of 50 mm and a height of 60 mm. This resulted in an L/D ratio of 1.2, the ratio of height to diameter of the samples. The dimension of sample has limited effects on the cyclic response of clayey soil under triaxial cyclic loading [20]. The height of the samples (corresponding to L/D ratio of 1.2) is similar to that used by some researchers [18] and greater than that of 50 mm (corresponding to L/D ratio of 1) used by some other researchers [20]. The samples were saturated under a back pressure of 300 kPa to obtain a Skempton's B-value of at least 0.96. The samples were isotropically consolidated to the effective confining pressure of 100 kPa, 150 kPa and 500 kPa to prepare normally and over consolidated samples. The cyclic loading was performed under the confining pressure of 100 kPa. So, the OCRs of the samples were 1, 1.5 and 5, respectively.

After consolidation, 10,000 sinusoidal loading cycles were applied to all samples under the loading frequency of 1 Hz. This loading frequency has been widely adopted to simulate traffic loading in previous studies [21]. In addition, the loading frequency of 1 Hz was also used in the previous study to investigate the cyclic deformation of clay under different drainage conditions [15]. One-way cyclic loading was used to simulate traffic loading where there was no cyclic tension. The loading waveform is shown in Fig. 2. Both UD and PD conditions were considered in this study. For the PD cyclic tests, only the drainage valve to the top surface was open to slow the drainage process. The pore pressure in the samples was monitored using a pore pressure transducer to the bottom surface. The cyclic deviatoric stress (peak to peak value) varied from 25 to 55 kPa. So, the ratio of cyclic stress to initial effective mean stress, namely the cyclic stress ratio (CSR), ranged from 0.25 to 0.55. The test schemes are summarized in Table 1. Samples are named based on the drainage condition, cyclic stress amplitude and OCR value. For

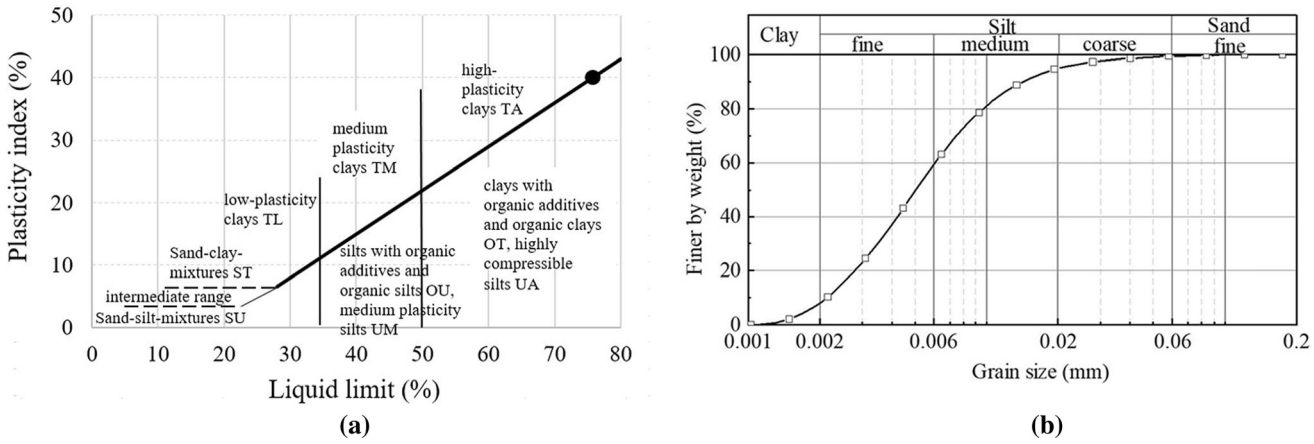

Fig. 1 **a** Position of the tested soil in the Casagrande diagram and **b** grain size distribution curve from a laser particle size analyser

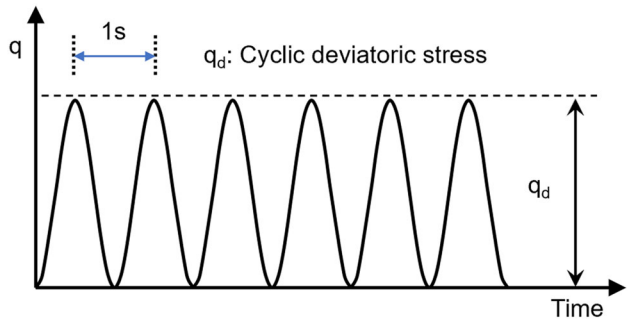

Fig. 2 The used loading waveform

example, PD-25-1.5 refers to the test under a PD condition with a cyclic stress amplitude of 25 kPa and OCR of 1.5. The effective mean stress (p') and deviatoric stress (q) are defined as follows:

$$p' = \frac{\sigma_1' + 2\sigma_3'}{3} \tag{1}$$

and

$$q = \sigma_1' - \sigma_3', \tag{2}$$

where σ_1' and σ_3' are the effective major and minor principal stresses, respectively.

3 Results and Discussions

This section presents and analyses the strain accumulation, EPWP and Mr of the samples subjected to different loading and drainage conditions.

Table 1 Cyclic triaxial tests series

Test ID	q_d (kPa)	CSR	OCR	Drainage condition
UD-25-1	25	0.25	1	UD
UD-30-1	30	0.3	1	UD
PD-25-1	25	0.25	1	PD
PD-30-1	30	0.3	1	PD
UD-25-1.5	25	0.25	1.5	UD
UD-30-1.5	30	0.3	1.5	UD
UD-35-1.5	35	0.35	1.5	UD
UD-40-1.5[a]	40	0.4	1.5	UD
PD-25-1.5	25	0.25	1.5	PD
PD-30-1.5	30	0.3	1.5	PD
PD-35-1.5	35	0.35	1.5	PD
PD-40-1.5	40	0.4	1.5	PD
UD-40-5	40	0.4	5	UD
UD-55-5	55	0.55	5	UD
PD-40-5	40	0.4	5	PD
PD-55-5	55	0.55	5	PD

q_d is cyclic stress; UD and PD refer to undrained and partially drained conditions, respectively

[a]Only 5822 loading cycles were applied due to the failure of the sample; CSR: the ratio of cyclic deviatoric stress to initial effective mean stress

3.1 Axial Strain and EPWP Accumulation

3.1.1 The Effects of Drainage Conditions on Strain Accumulation

The accumulated axial strain is normally greater PD condition than under UD condition except the samples with OCR = 1.5 and CSR = 0.4 as shown in Fig. 3. For other samples as shown in Fig. 3a, b, d, the accumulative axial strains after 10,000 loading cycles are about 0.96%, 0.12%,

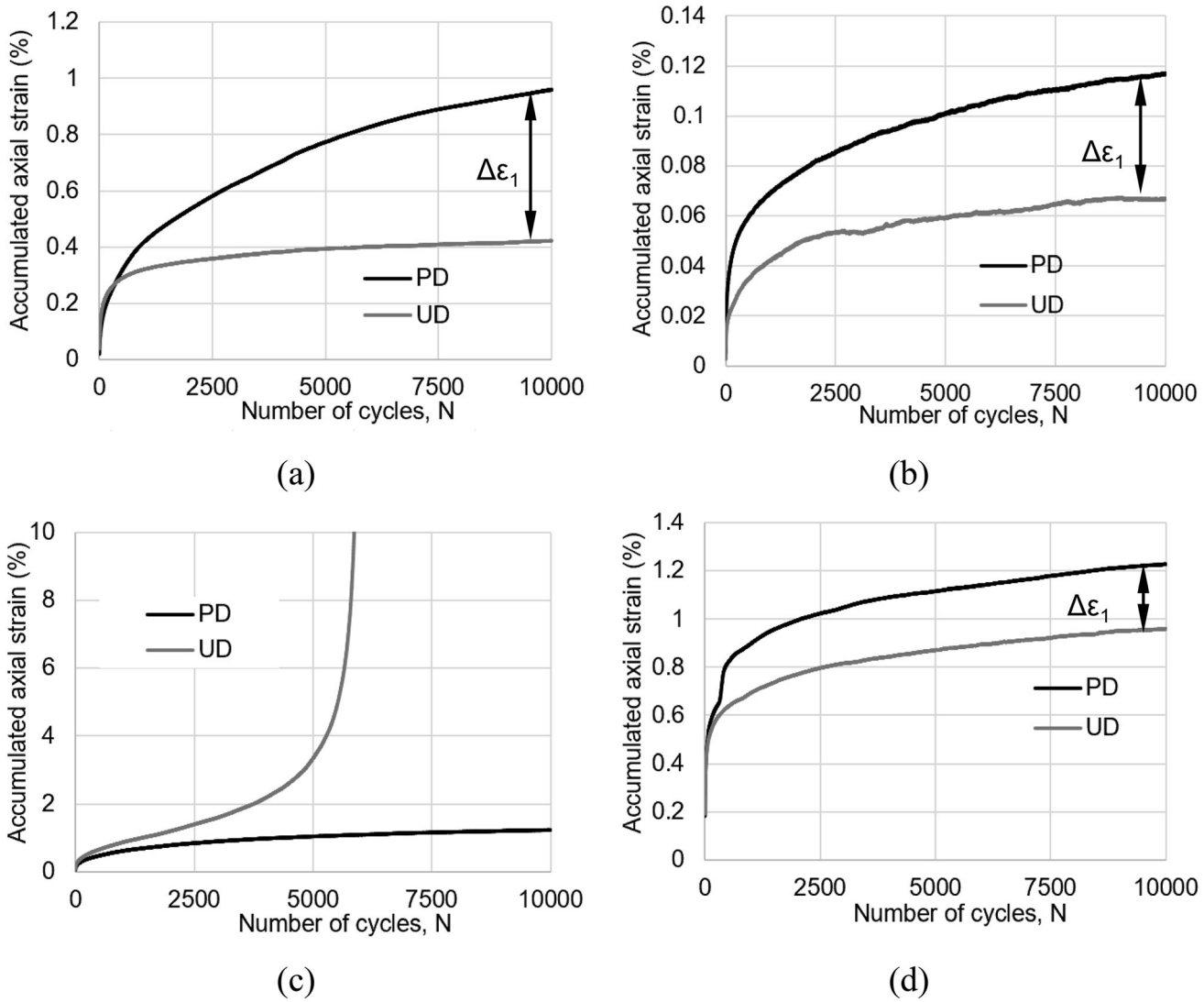

Fig. 3 The accumulated axial strain accumulation under **a** OCR = 1, CSR = 0.3; **b** OCR = 1.5, CSR = 0.3, **c** OCR = 1.5, CSR = 0.4 and **d** OCR = 5, CSR = 0.55

and 1.22% under PD condition. But the values are about 0.42%, 0.07% and 0.96%, respectively, under UD condition. Such a phenomenon can be better seen in Fig. 4a which summarized the accumulated axial strain under PD and UD conditions. Figure 4b reveals the accumulative axial strain differences ($\Delta\varepsilon_1$) between samples under the PD and UD conditions. It shows that larger cyclic stress ratios lead to greater differences. For example, for the samples with OCR = 1.5, the $\Delta\varepsilon_1$ increases from 0.049 to 0.13% when the CSR increases from 0.25 to 0.35.

Some samples may fail under UD condition but remain intact under PD condition. This can be seen in the samples UD-40-1.5 and PD-40-1.5 (see Fig. 3c). The accumulative axial strain is over 10% in the sample UD-40-1.5 after 5822 cycles under UD condition but is only about 1.2% in the sample PD-40-1.5 after 10,000 loading cycles under PD condition. This may be due to the rapid development of EPWP in the sample under UD condition as discussed later.

The amplitude of traffic loading is rather small, which leads to soil deformation but not failure [22]. Under such a small cyclic stress amplitude, the axial strain accumulation under PD condition is greater than that under UD condition as shown in Figs. 3 and 4. A similar phenomenon was also reported on normally consolidated clay with even more loading cycles (30,000 loading cycles) under the same loading frequency of 1 Hz [15]. This means that traditional UD cyclic tests on clayey soil may underestimate its deformation under long-term traffic loading, and PD condition should be considered when analysing the long-term deformation of geotechnical infrastructures in normally or over consolidated clayey soil. This compensates the finding on normally consolidated clayey soil [15].

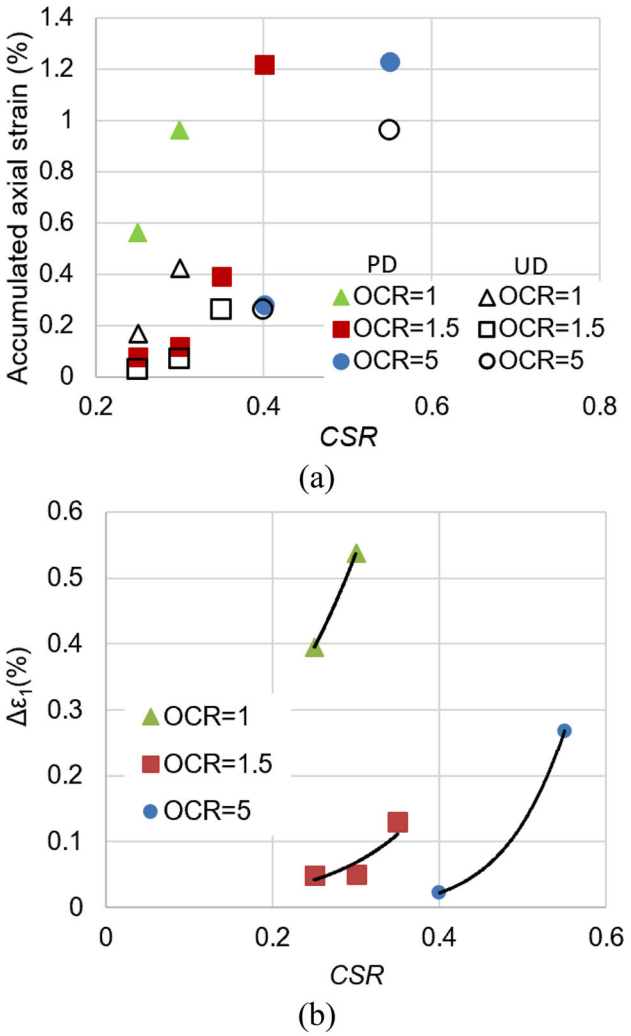

Fig. 4 The comparison of accumulated axial strain under PD and UD conditions, **a** the accumulated axial strain and **b** the difference of axial strain under different drainage conditions

3.1.2 The effects of OCR and CSR on strain accumulation

OCR has significant effects on strain accumulation as shown in Fig. 4a. Under the same CSR, the greater the OCR value, the less the strain accumulation for both UD and PD conditions. For example, the axial strain is about 0.96% in the sample PD-30-1, whilst it is only 0.12% in the sample PD-30-1.5 under the same cyclic stress of 30 kPa. This is consistent with the finding that compared with normally consolidated soil, much less strain accumulation was observed in slightly over consolidated soil [11, 23].

Under the same OCR, more axial strains accumulate as CSR increases. For example, at OCR = 1.5, the sample UD-40-1.5 failed after 5822 cycles as discussed earlier. But the soils with OCR = 5 have not failed even under loading with higher CSR. The accumulative axial strains in the samples with the OCR = 5 are in the range of 0.96–1.23% under higher CSR (e.g. 0.55) as shown in Fig. 4b. These values are far from the failure strain of 5% suggested in the previous study [24]. Such phenomena suggest that increasing OCR value would increase the failure resistance of the soil under cyclic loading. This is because over consolidation would lead to the development of soil fabric, densification and greater UD shear strength [25].

3.1.3 Accumulation of EPWP

The EPWP in the samples accumulates under different rules as revealed in Fig. 5. The accumulation of EPWP is greatly affected by drainage conditions, OCR and CSR. Under UD condition, the EPWP accumulation rate reduces with OCR for a given CSR. For both samples with CSR = 0.3 (Fig. 5a, b), the EPWP increases quickly in the first few loading cycles, but the rate is much higher in the sample with lower OCR = 1. The EPWP reaches 20 kPa within 500 loading cycles in the sample of OCR = 1, but only 4 kPa in the sample of OCR = 1.5. The EPWP keeps increasing at a diminishing rate to about 37 kPa after 10,000 cycles in the sample of OCR = 1. But the EPWP stabilizes at 4 kPa after about 1,000 cycles in the sample of OCR = 1.5. This explains the lower accumulative strains observed in the samples with higher OCRs as discussed earlier.

Furthermore, for the sample UD-40-1.5, the EPWP accumulates greatly and is over 75 kPa after 5822 cycles, which is much greater than that in the sample UD-30-1.5 (see Fig. 5b, c). If OCR increases to 5, higher EPWP accumulates under CSR = 0.55 compared to that in the sample with OCR = 1.5 and CSR = 0.3 (see Fig. 5b, d). This suggests that increasing CSR increases the rate of EPWP accumulation under UD condition. This is the same for PD condition as discussed below.

Under PD condition, the EPWP accumulation rates in the early cyclic loading stage are the same as those under UD condition as shown in Fig. 5. But under PD condition, the EPWP starts to decrease after a number of loading cycles as the dissipation rates over passing the accumulation rates. A similar variation in EPWP under PD condition was also observed on Ariake silty clay [16, 17].

The dissipation of EPWP would result in higher effective mean stresses in the samples under PD condition than those under UD condition. However, the axial strain accumulation under PD condition is noticeably greater than that under UD condition as shown in Figs. 1 and 2. This contradicts the findings that applying a smaller confining pressure results in greater strain accumulation [26]. This is because the deformation mechanism of soil under drained conditions is different from that soil under drainage conditions. Under UD condition, the accumulation of strain is due to the adjustment of microstructure under cyclic

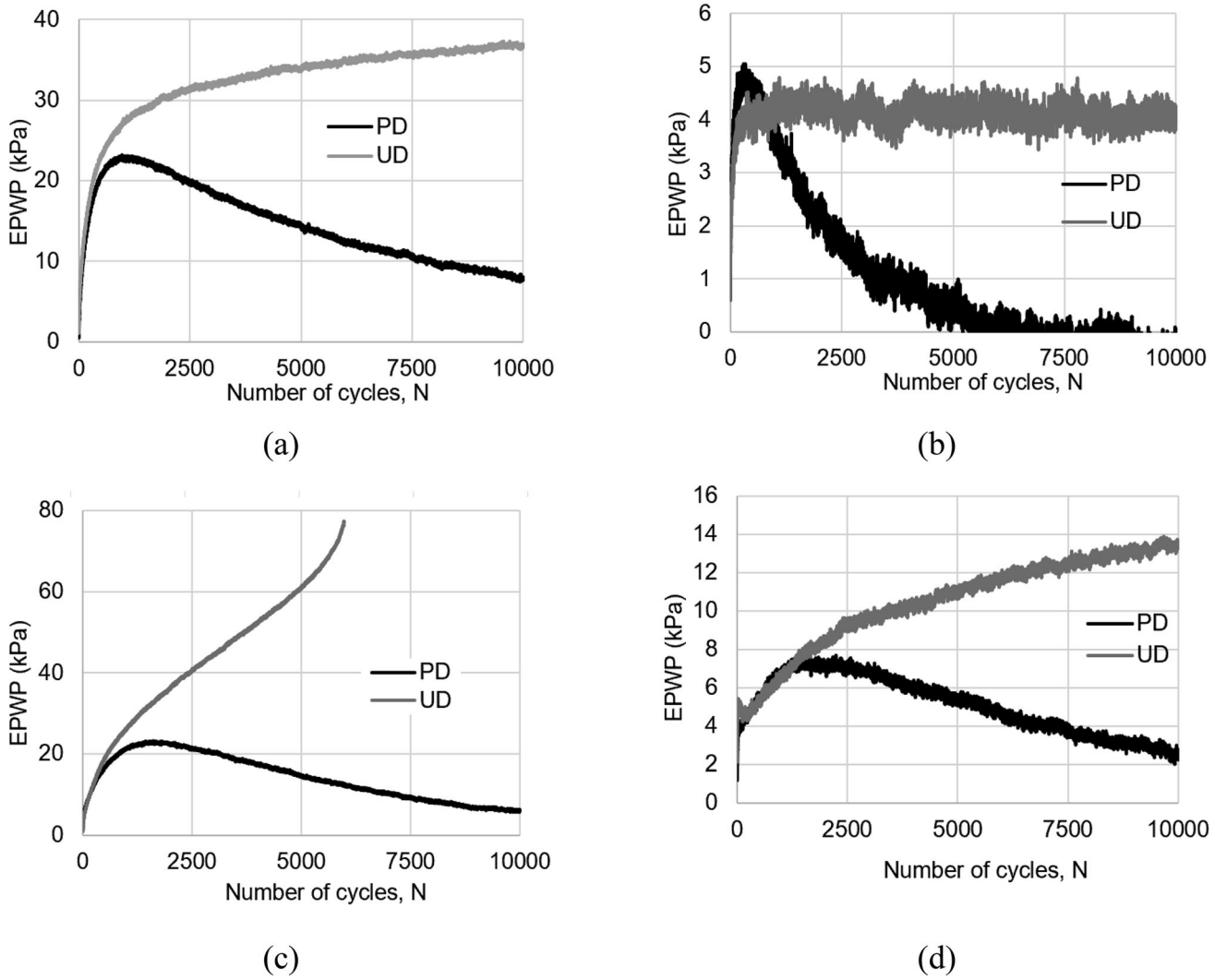

Fig. 5 The accumulated EPWP under **a** OCR = 1, CSR = 0.3; **b** OCR = 1.5, CSR = 0.3; **c** OCR = 1.5, CSR = 0.4 and **d** OCR = 5, CSR = 0.55

loading such as particle sliding or rotation [27]. However, under PD condition, in addition to the adjustment of microstructure induced deformation, the dissipation of EPWP would cause additional consolidation deformation. This causes the accumulative axial strain under PD condition greater than that under UD condition as shown in Fig. 3. Such a phenomenon suggests that effective confining pressure or stress state in a sample is not the sole factor influencing strain accumulation. The drainage conditions are also important as the deformation mechanisms are different.

Figure 6 compares the accumulative EPWP at the end of the tests in the UD tests. Similar to the axial strain, much less EPWP accumulated in the samples with greater OCRs. For example, under the CSR of 0.3, EPWP is about 37 kPa in the normally consolidated sample, while it is just 4.2 kPa in the sample with OCR = 1.5. This is because the sample with higher OCR has a lower void ratio and lower

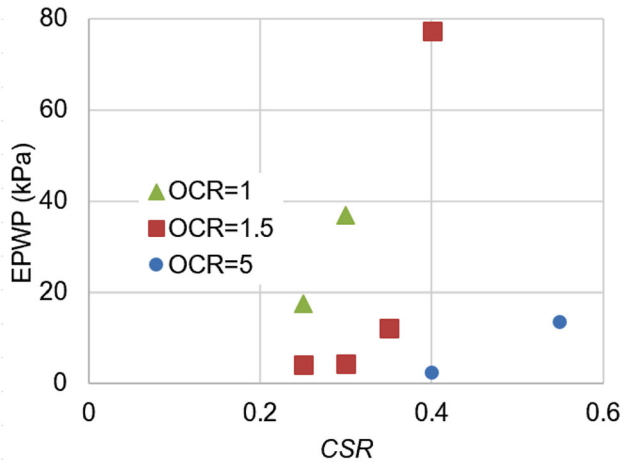

Fig. 6 The EPWP in the samples subjected to different CSRs under UD condition

compressibility, which leads to less EPWP under the same CSR.

Figure 7 shows the relationship between the accumulative axial strain and the EPWP normalized by the initial effective mean stress (100 kPa) in UD condition. Under the same normalized EPWP, strain accumulation is greater in the sample with a higher OCR value. For example, when the normalized EPWP is about 0.12, the accumulative axial strain is about 0.26% in the sample with OCR = 1.5 (CSR = 0.35), but the respective values are 0.13 and 0.96% in the sample with OCR = 5 (CSR = 0.55). This can also be seen in the variation of volumetric strains in the PD samples as discussed later. This means that for over consolidated soil, axial strain would accumulate greatly with little EPWP accumulation, particularly in heavily over consolidated soil. This suggests that the sample with a higher OCR value shows greater dilatancy.

3.2 The Volumetric Strain Accumulation

Under PD condition, volumetric strain accumulates due to the dissipation of EPWP. Figure 8 shows the accumulative volumetric strain in samples under different loading conditions. For the soil with the same OCR, applying greater cyclic stress leads to greater volumetric strain accumulation, as greater cyclic stress leads to greater mean total stress.

In addition, OCR has significant effects on the volumetric strain. The greater the OCR, the less the volumetric strain accumulates after 10,000 loading cycles. For example, under the CSR of 0.4, the volumetric strain accumulates about 0.93% in the sample with OCR = 1.5, while it is just about 0.05% under an OCR of 5. This is because the samples with greater OCR values have a smaller void ratio and greater densification, so less volumetric deformation

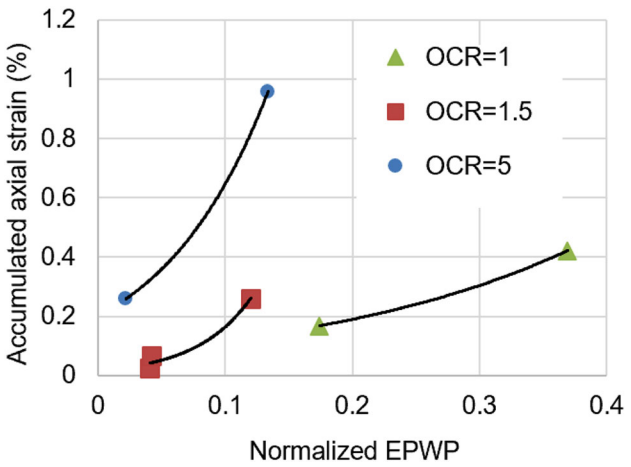

Fig. 7 The relationship between axial strain and EPWP in the samples under UD condition

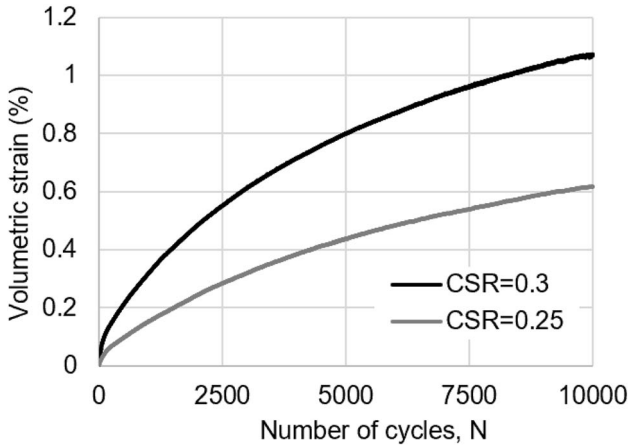

(a)

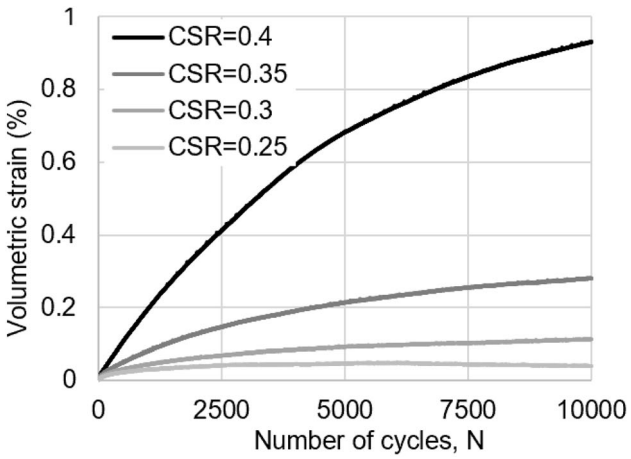

(b)

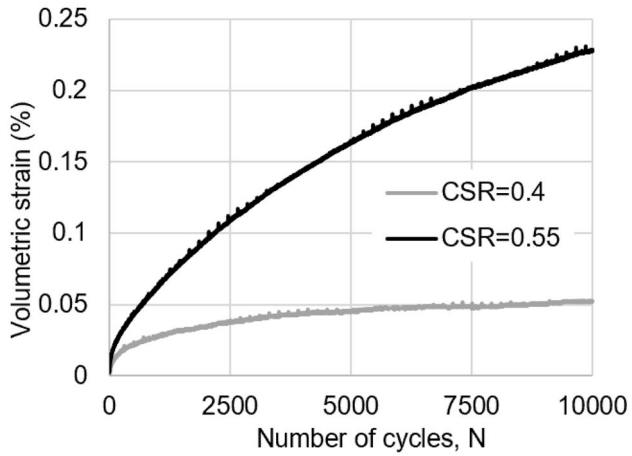

(c)

Fig. 8 The accumulated volumetric strain under different CSR, **a** OCR = 1; **b** OCR = 1.5 and **c** OCR = 5

occurs under cyclic loading. This is consistent with the finding in EPWP under UD condition as discussed earlier.

In triaxial tests, lateral strain (ε_3) can be estimated using

$$\varepsilon_3 = \frac{\varepsilon_v - \varepsilon_1}{2}, \tag{3}$$

where ε_v and ε_1 refer to volumetric and axial strains, respectively. The lateral deformation may not be uniform in samples under PD condition, as the degrees of consolidation vary along the depth of the samples. Still, Eq. (3) can be used to estimate the average lateral deformation [16]. Under constant-volume test conditions (UD condition), Eq. (3) becomes

$$\varepsilon_3 = -\frac{\varepsilon_1}{2}. \tag{4}$$

In Eqs. (3) and (4), a negative value in ε_3 suggests lateral bulging and a positive value means lateral contraction.

Figure 9 reveals the development of lateral strain accumulation under different testing conditions. The lateral deformation is affected by CSR, OCR and drainage conditions. Under the same OCR, applying a greater CSR leads to larger lateral strain accumulation. For example, in the samples with OCR = 1, the lateral strains after 10,000 loading cycles are about 0.03% and 0.06% under the CSRs of 0.25 and 0.3, respectively.

OCR could affect the development pattern of lateral strains. Under UD condition, the samples expand laterally as loading continues, and the deformation is not affected by CSR. For samples under PD condition, the lateral deformation starts with contraction and then could expand or not depending on the OCR. For the samples with OCR = 1 and OCR = 1.5, as shown in Fig. 9, lateral strain starts at negative values, indicating a bulging behaviour initially. The greater the OCR and CSR values, the greater the lateral expansion is. Depending on the OCR values, the sample could contract laterally after reaching certain deformation levels, and the lower the OCR value, the greater the contraction. For example, when OCR = 1 and CSR = 0.3, the sample starts to contract when the lateral strain reaches about $\varepsilon_3 = -0.055\%$. But when OCR = 5, no contraction behaviour can be observed.

The different lateral deformation behaviours in the samples observed above are mainly caused by the different responses in EPWP to cyclic loading. Under PD condition, in the early loading stage, the EPWP dissipation rate is lower than its accumulation rate. Therefore, the EPWP accumulation tendency is similar to that under UD condition (see Fig. 5). The effective stress decreases as EPWP increases. This leads to the bulging of the samples under cyclic shear. The lower the OCR, the greater the accumulated EPWP is (see Fig. 5) and so is the lateral bulging. Once the EPWP dissipation rate exceeds the accumulation

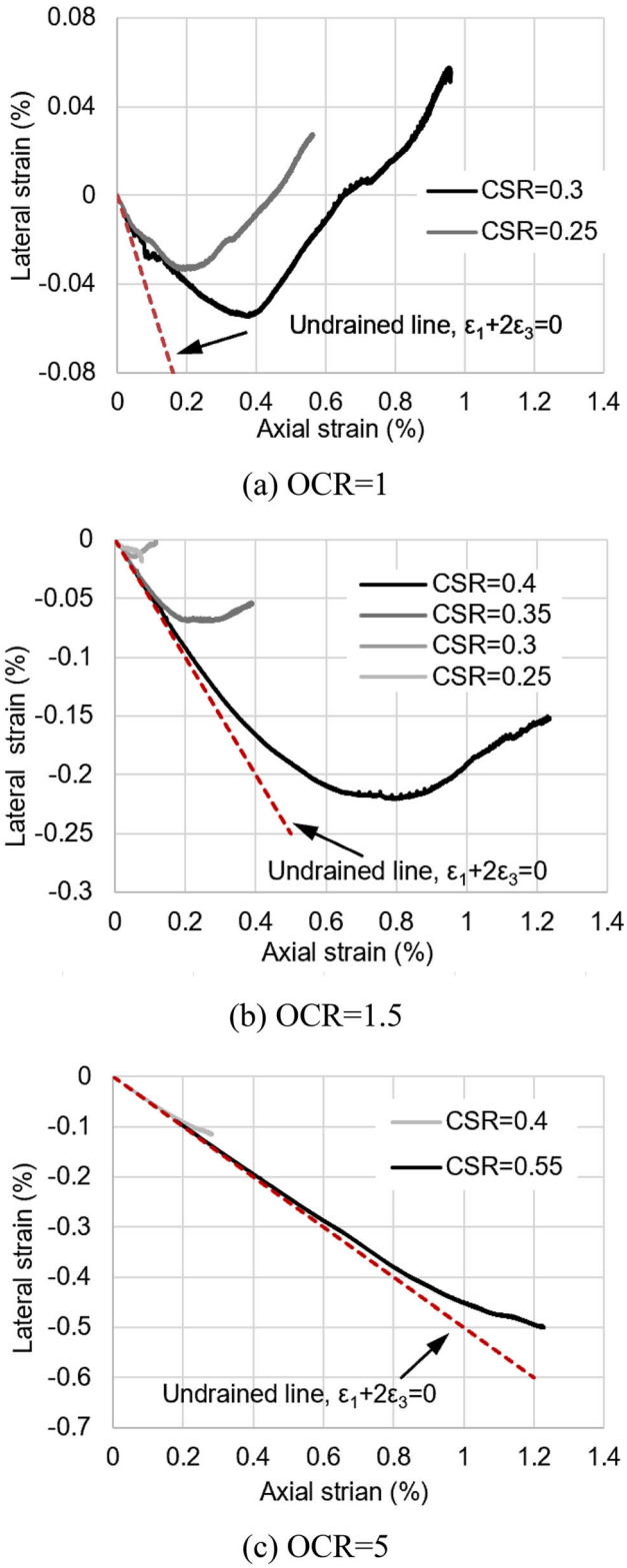

Fig. 9 The relationship between lateral and axial strain under PD condition

rate, the EPWP starts to decrease under PD condition. So the sample starts to consolidate and contract laterally. Once the volumetric strain is greater than the axial strain, as expected from Eq. (3), the lateral strain becomes positive as shown in Fig. 9a, suggesting that the sample shows contraction in both axial and lateral directions.

The contraction behaviour observed in the samples with lower OCR values is very different from that under UD condition where the lateral deformation is always bulging. Such a phenomenon means that reconsolidation greatly contributes to the deformation of soil. Therefore, the strain accumulation under PD condition could be much greater than that under UD condition. For over consolidated soils, the partial drainage conditions can be ignored if the duration of cyclic loading is not long enough for consolidation to occur.

For the samples with OCR = 5, the lateral strain accumulation follows that of the sample under UD condition even under high CSR values as revealed in Fig. 9c. This can be also found in the accumulative axial strain as shown in Fig. 4. For example, of the samples with OCR = 5, the axial strain accumulations under PD condition are only about 8–22% greater than those under UD condition after 10,000 loading cycles, while the difference is much more significant in normally consolidated soil shown in Fig. 4b.

Figure 10a illustrates the lateral strain accumulation against axial strain after 10,000 loading cycles. It shows that if the OCR of soil is high enough, it is acceptable to neglect the partial drainage condition if the number of loading cycles and the CSR are not too large. For the normally consolidated soil, e.g. OCR = 1, however, using UD cyclic loading test results may misinterpret the behaviour of the soil under PD condition.

Figure 10b reveals the relationship between accumulative axial strain with volumetric strain. As can be seen, for both normally and over consolidated samples, axial strains increase with the development of volumetric strain accumulation. However, for the samples with greater OCR, the greater axial strain could accumulate with the same development in volumetric strain. For example, as estimated from the figure, with the volumetric strain accumulation of about 0.2%, the axial strain develops about 1% in the sample with an OCR of 5, while it is only about 0.25% at an OCR of 1.5. This is consistent with the lower EPWP development in the samples with greater OCR under UD condition as shown in Fig. 7. This means that for the over consolidated soil under PD condition, the reconsolidation induced deformation only has a minor contribution to the axial strain accumulation. The main contribution could be the adjustment of microstructure induced by cyclic loading and/or cyclic loading induced destruction of soil fabric developed in the consolidation stage. This will be discussed below together with the variation of Mr.

3.3 The variation of Mr

The resilient modulus (Mr) of the soil is calculated based on Fig. 11. Figure 12 reveals the variation of Mr in the samples under different loading conditions. Similar to strain accumulation, the Mr is affected by drainage conditions, OCR and CSR. Under both UD and PD conditions, the Mr increase with OCR at given CSRs and decrease with CSR at given OCRs. For example, at CSR of 0.25, the resilient moduli during the first loading cycle in the samples with OCR = 1 and 1.5 under UD condition are about 39.4 MPa and 62.4 MPa, respectively (see Fig. 12a, b).

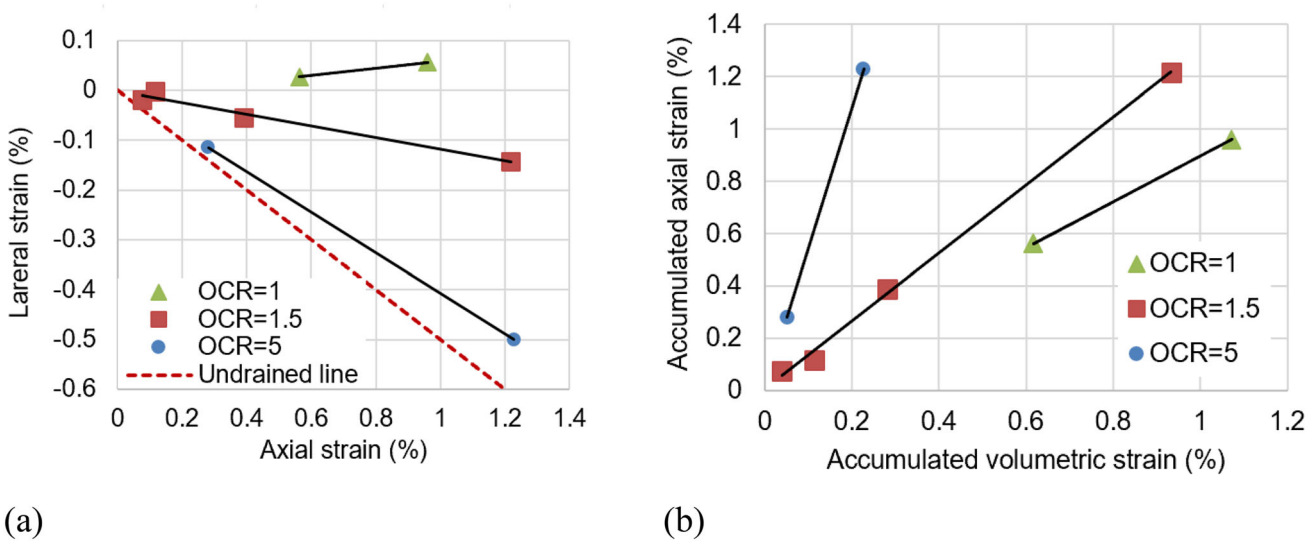

Fig. 10 The relationship between: **a** lateral and axial strains; **b** axial and volumetric strains of samples with different OCR under PD condition

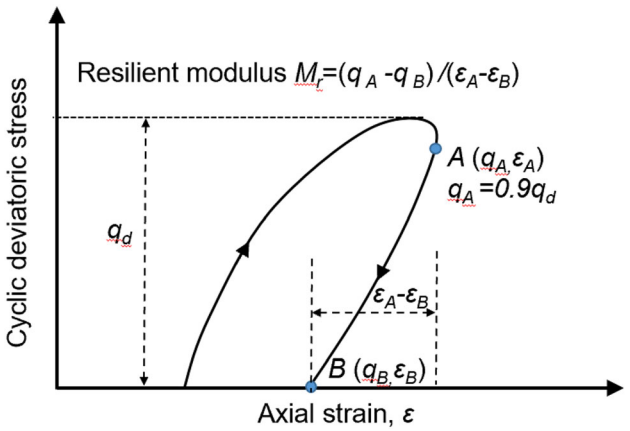

Fig. 11 The definition of Mr [18]

The respective values are 37.8 MPa and 32.4 MPa in the samples with OCR = 5 under CSR of 0.4 and 0.55 as shown in Fig. 12c.

Under UD condition, the Mr decreases with the increases in loading cycles as shown in Fig. 12a–c. Particularly, in the sample UD-40-1.5, the Mr degrades greatly, suggesting an almost total loss of stiffness and instability under the UD condition. One possible cause is the accumulation of EPWP as shown in Fig. 5a. This causes a decrease in the effective mean stress as cyclic loading continues. The result is consistent with the findings reported by Liu et al. [18] that the Mr of normally consolidated soil decreases with effective mean stress. However, for the sample with OCR = 1.5 and CSR = 0.25 (UD-25-1.5), a small increase in Mr is observed as loading continues. This may be attributed to the small stress–strain behaviour of soil and/or the adjustment of microstructure [11, 18].

Though the degradation in stiffness shows dependence on EPWP, the variation is affected by OCRs. As shown in Fig. 6, for the samples with OCR of 5, there is very limited EPWP accumulated under UD condition, but the Mr degrades significantly as shown in Fig. 12c. This means that the degradation of stiffness may not be solely attributed to the change of effective mean stress. This can be better seen in Fig. 13a which shows the relationship of the stiffness ($Mr_{N=10,000}$) during the 10,000th loading cycle with the accumulated EPWP under different OCR values. The stiffness is normalized by the Mr ($Mr_{N=1}$) during the first loading cycle and EPWP is normalized by the initial effective mean stress (100 kPa). As can be seen, the stiffness reduces with the normalized EPWP, but the samples with OCR = 5 show a greater change in stiffness with a little EPWP accumulation. For example, in the samples UD-55-5 and UD-35-1.5 with the normalized EPWPs at both about 0.13, the stiffness degrades by 56% in the sample UD-55-5 after 10,000 loading cycles, whilst it degrades by only 25% in the sample UD-35-1.5. This means that the change in effective mean stress alone cannot explain the degradation of stiffness in over consolidated soil.

The degradation of stiffness of over consolidated soil may be attributed to the destruction of soil fabric developed in the consolidation stage. Soil fabric may develop during the consolidation stage in soils [25]. Under cyclic loading, particularly if the cyclic stress amplitude is great enough, the soil fabric can be destructed, resulting in a loss in stiffness. This leads to great axial strain accumulation. And the stiffness of soil degrades significantly without too much change in EPWP under UD condition as revealed in Fig. 13a.

Under PD condition, however, as shown in Fig. 12d, e, the resilient moduli in the samples with OCR = 1 and 1.5 decrease within certain loading cycles and then increase gradually as cyclic loading continues. For the samples with an OCR of 5, as shown in Fig. 12f, as cyclic loading continues, the stiffnesses decrease first and then show little change afterwards. Such variation in the stiffness under PD condition is different from that under UD condition. This is because, as discussed earlier, under PD condition EPWP develops during the early loading stage and then dissipates as cyclic loading continues. So, the effective mean stress decreases first and then increases afterwards. In addition, as cyclic loading continues, the existing soil fabric in samples has been damaged, resulting in a loss of stiffness. On the other hand, as cyclic loading continues, volumetric strain develops gradually as shown in Fig. 8. This induces a new densification process in the sample and a reduction in the void ratio, which contributes to the increase in Mr.

Figure 12f shows that the stiffness of the sample UD-55-5 decreases by 37% from 31.7 to 20 MPa after 2500 loading cycles. However, the maximum EPWP observed in the sample is only about 7 kPa as shown in Fig. 5d. In addition, under the over consolidation ratio of 5 and UD condition, Mr degrades about 20–55% with EPWP accumulation of 2–13 kPa. This also suggests that the destruction of soil fabric rather than the reduction in effective mean stress is the main cause of the degradation in the stiffness of over consolidated soils. Since the volumetric strains in the samples with OCR = 5 and CSR = 0.4 is small as shown in Fig. 8c, limited densification has been introduced in the sample. Therefore, there is little variation in the stiffness of the sample under cyclic loading as shown in Fig. 12f.

Similarly, under PD condition, as shown in Fig. 13b, the Mr shows a decrease with volumetric strain accumulation and the samples with greater OCR experience greater degradation in stiffness under the same volumetric deformation. For example, in the sample PD-35-1.5, the volumetric strain is about 0.28% and the stiffness degrades by

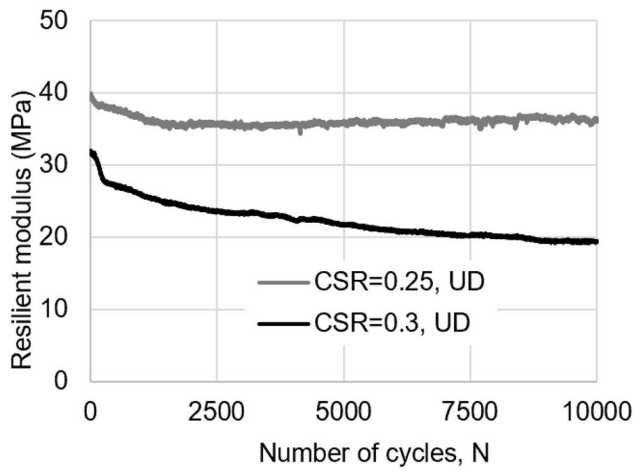

(a) OCR=1, UD

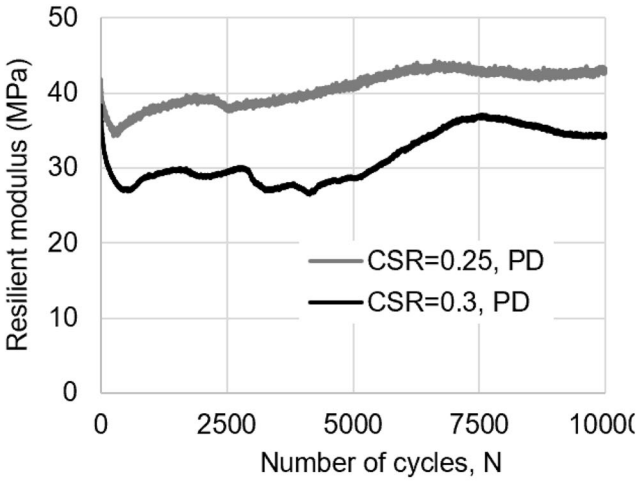

(d) OCR=1, PD

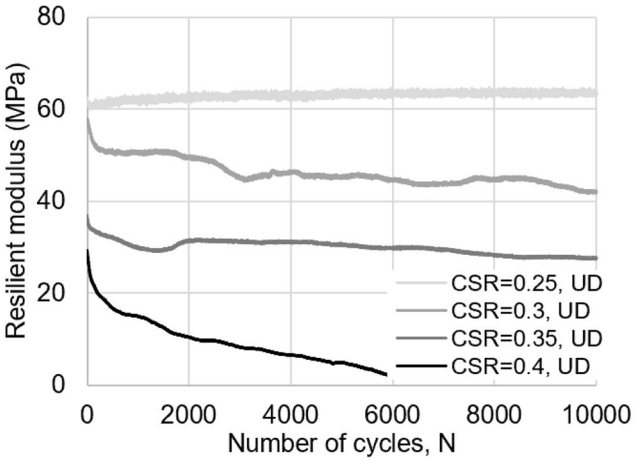

(b) OCR=1.5, UD

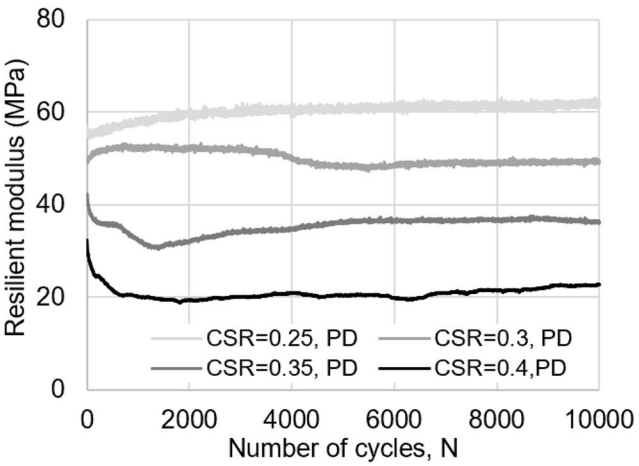

(e) OCR=1.5, PD

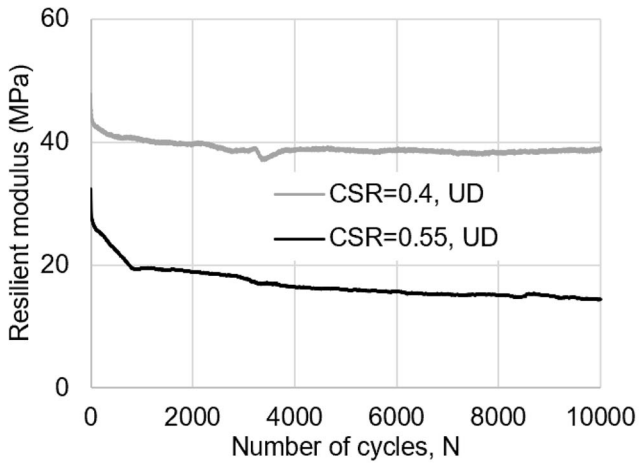

(c) OCR=5, UD

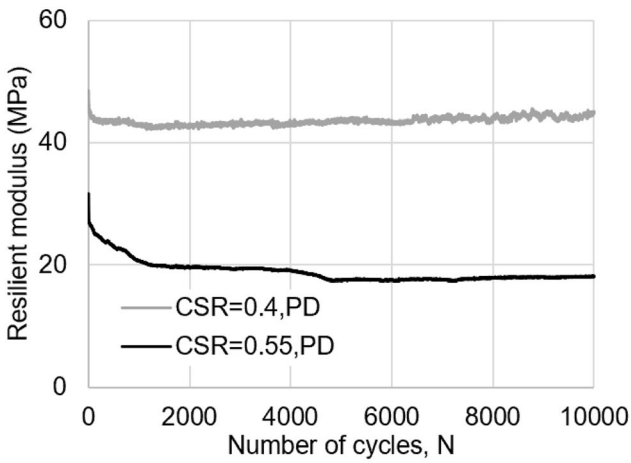

(f) OCR=5, PD

Fig. 12 The Mr under different CSR

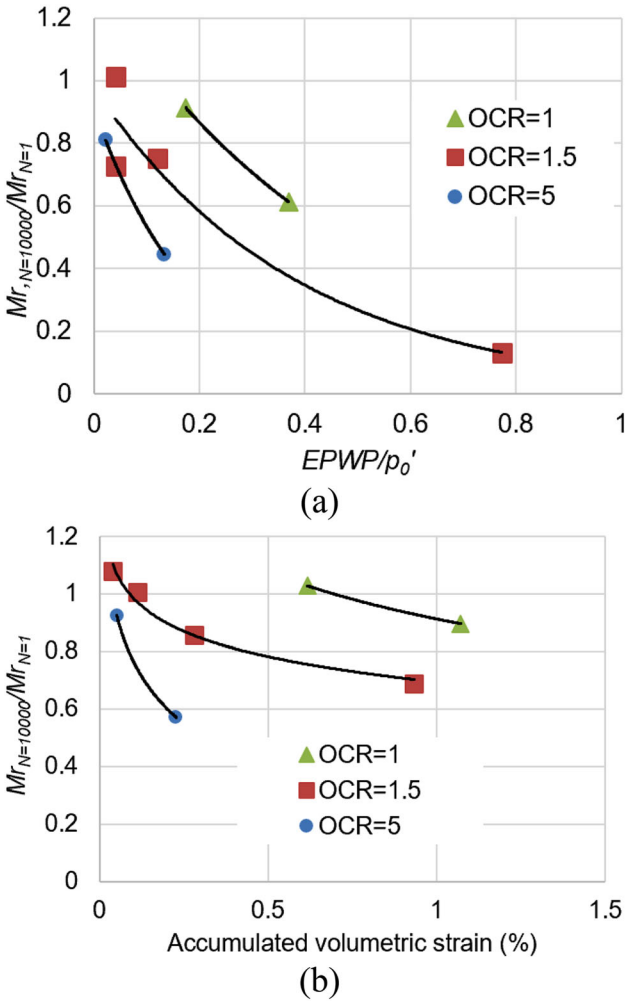

Fig. 13 **a** The relationship of Mr against EPWP under UD condition and **b** the relationship of Mr against accumulated volumetric strain under PD condition, $Mr_{,N=10,000}$ and $Mr_{,N=1}$ refer to the resilient moduli during the 10,000th and 1st loading cycles, respectively

about 14% from 42.1 to 36.2 MPa after 10,000 loading cycles. In contrast, the sample PD-55-5 experienced less volumetric strain (about 0.23%) but greater degradation in stiffness (about 43% from 31.7 MPa to 18.1 MPa). This is because the sample with larger OCR shows greater stress-dilatancy, and less volumetric strain can be observed even with greater damage in soil fabric.

4 Summary and Conclusions

A series of undrained and partially drained cyclic triaxial tests were performed on kaolin samples with different over consolidation ratios. The objectives are to investigate the effects of drainage condition, over consolidation ratio and cyclic stress ratio on the cyclic deformation behaviour of the soil. The accumulative axial strain, EPWP, volumetric strain accumulation and resilient modulus (Mr) of the soil are presented and discussed. The results of the tests indicate the following:

1. Under PD condition, due to reconsolidation deformation, the accumulative axial strain in both the normally and over consolidated soil under lower cyclic stress ratios (not a failure case) is greater than that under UD condition.
2. Under PD condition, with the increase of over consolidation ratio, the average lateral deformation is similar to that under UD condition.
3. The over consolidated ratio affects the relationship between the accumulative axial strain and EPWP under UD condition. It also affects the relationship between the accumulative axial strain and volumetric strain under PD condition. As the over consolidation ratio increases, greater axial strain could accumulate without too much accumulative EPWP or volumetric strain.
4. The Mr of soil decreases with the increase of EPWP in UD condition or volumetric strain accumulation under PD condition. For the heavily consolidated soil (for example, an over consolidation ratio of 5), the Mr degrades significantly with little accumulation in EPWP under UD condition or in volumetric strain under PD condition. This may be because the degradation of stiffness of the over consolidated soil is primarily attributed to the destruction of soil fabric developed in the consolidation stage.

Acknowledgements The project is funded by the ARC Industrial Transformation Research Hub Project Grant- IH180100010 (Project No. IH18.09.1), the National Natural Science Foundation of China (No.51968005), Guangxi Natural Science Foundation (No. 2019GXNSFBA185038) and Innovation Project of Guangxi Graduate Education (YCSW2022073).

Declarations

Conflict of interest The authors declare no commercial or associative interest that represents a conflict of interest in connection with the work submitted.

References

1. Shan Y, Meng QL, Yu SM, Mo HH, Li YD (2020) Energy based cyclic strength for the influence of mineral composition on artificial marine clay. Eng Geol 274:105713
2. Shan Y, Wang X, Cui J, Mo HH, Li YD (2021) Effects of clay mineral composition on the dynamic properties and fabric of artificial marine clay. J Mar Sci Eng 9(11):1216
3. Shan Y, Mo HH, Yu SM, Chen JS (2016) Analysis of the maximum dynamic shear modulus and particle arrangement properties of saturated soft clay soils. Soil Mech Found Eng 53(4):226–232

4. Yu S, Shan Y (2017) Experimental comparison and study on small-strain damping of remolded saturated soft clay. Geotech Geol Eng 35(5):2479–2483
5. Shan Y, Chen J, Ke X, Mo HH (2019) Resonant column test study of the effect of clay minerals on maximum dynamic shear modulus in marine clay. In: Proceedings of the 7th international conference on earthquake geotechnical engineering. CRC Press, Rome
6. Liu Z, Xue J (2021) The deformation characteristics of a kaolin clay under intermittent cyclic loadings. Soil Dyn Earthq Eng 153:107112
7. Pan K, Liu XM, Yang ZX, Jardine RJ, Cai YQ (2021) Undrained cyclic response of K-0-consolidated stiff cretaceous clay under wheel loading conditions. J Geotech Geoenviron Eng 147:04021087
8. Wang J, Ming D, Cai Y, Guo L, Du Y, Wang C (2021) Influences of initial static shear stress on the cyclic behaviour of over consolidated soft marine clay. Ocean Eng 224:108747
9. Wang Y, Zeng C, Jia HY, Cai HJ, Zhang XY (2019) Cyclic behavior of natural organic clay under variable confining pressure that match traffic loading condition. Mar Georesour Geotechnol 37(3):402–407
10. Shi W, Wang J, Guo L, Hu X, Fu H, Jin J, Jin F (2018) Undrained cyclic behavior of over consolidated marine soft clay under a traffic load-induced stress path. Mar Georesour Geotechnol 36:163–172
11. Qian J, Li S, Zhang J, Jiang J, Wang Q (2019) Effects of OCR on monotonic and cyclic behavior of reconstituted Shanghai silty clay. Soil Dyn Earthq Eng 118:111–119
12. Han J, Yin ZY, Dano C, Hicher PY (2021) Cyclic and creep combination effects on the long-term UD behavior of overconsolidated clay. Acta Geotech 16:1–15
13. Dai M, Guo L, Li M, Jin T (2021) The pore pressure generation and deformation of overconsolidated soft marine clay considering initial static shear effect. Mar Georesour Geotechnol. https://doi.org/10.1080/1064119X.2021.1951406
14. Mamou A, Powrie W, Priest JA, Clayton C (2017) The effects of drainage on the behaviour of railway track foundation materials during cyclic loading. Géotechnique 67:845–854
15. Guo L, Liu L, Wang J, Jin H, Fang Y (2020) Long term cyclic behavior of saturated soft clay under different drainage conditions. Soil Dyn Earthq Eng 139:106362
16. Sakai A, Samang L, Miura N (2003) Partially-drained cyclic behavior and its application to the settlement of a low embankment road on silty-clay. Soils Found 43:33–46
17. Hyodo M, Yasuhara K, Hirao K (1992) Prediction of clay behaviour in undrained and partially drained cyclic triaxial tests. Soils Found 32:117–127
18. Liu Z, Xue J, Mei G (2021) The impact of stress disturbance on undrained cyclic behaviour of a kaolin clay and settlement of tunnels under cyclic loading. Acta Geotech 16:3947–3961
19. GB/T 50124-1999 (1999) Standard for soil test method. Beijing, China: Ministry of Construction of the People's Republic of China
20. Wichtmann T, Andersen KH, Sjursen MA, Berre T (2013) Cyclic behaviour of high-quality undisturbed block samples of Onsøy clay. Can Geotech J 50(4):400–412
21. Yang Q, Tang YQ, Yuan B, Zhou J (2019) Cyclic stress-strain behaviour of soft clay under traffic loading through hollow cylinder apparatus: effect of loading frequency. Road Mater Pavem Des 20:1026–1058
22. Ren XW, Xu Q, Teng JD, Zhao N, Lv L (2018) A novel model for the cumulative plastic strain of soft marine clay under long-term low cyclic loads. Ocean Eng 149:194–204
23. Liu Z, Xue J (2021) The deformation behaviour of an anisotropically consolidated kaolin clay under lateral cyclic loading. Mar Georesour Geotechnol. https://doi.org/10.1080/1064119X.2021.2002986
24. Yang J, Sze HY (2011) Cyclic behaviour and resistance of saturated sand under non-symmetrical loading conditions. Géotechnique 61(1):59–73
25. Price AB, DeJong JT, Boulanger RW (2017) Cyclic loading response of silt with multiple loading events. J Geotech Geoenviron Eng 143:04017080
26. Thakur PK, Vinod JS, Indraratna B (2013) Effect of confining pressure and frequency on the deformation of ballast. Géotechnique 63:786–790
27. Qian JG, Wang YG, Yin ZY, Huang MS (2016) Experimental identification of plastic shakedown behavior of saturated clay subjected to traffic loading with principal stress rotation. Eng Geol 214:29–42
28. Chai JC, Miura N (2002) Traffic-load-induced permanent deformation of road on soft subsoil. J Geotech Geoenviron Eng 128:907–916
29. Chazallon C, Hornych P, Mouhoubi S (2006) Elastoplastic model for the long-term behavior modeling of unbound granular materials in flexible pavements. Int J Geomech 6:279–289
30. Ishihara K (1996) Soil behavior in earthquake geotechnics. Clarendon Press, Oxford
31. Liu Z, Xue J, Yaghoubi M (2021) The effects of unloading on undrained deformation of a kaolin clay under cyclic loading. Soil Dyn Earthq Eng 140:106434
32. Qian J, Wang Q, Jiang J, Cai Y, Huang M (2018) Centrifuge modelling of a saturated clay ground under cyclic loading. Int J Geomech 18:04018041
33. Sun L, Cai Y, Gu C, Wang J, Guo L (2015) Cyclic deformation behaviour of natural K0-consolidated soft clay under different stress paths. J Cent South Univ 22:4828–4836
34. Tatsuya I, Sekine E, Miura S (2011) Cyclic deformation of granular material subjected to moving-wheel load. Can Geotech J 48:691–703
35. Wang Y, Wan Y, Wan E, Zhang X, Zhang B, Zhong Y (2021) The pore pressure and deformation behavior of natural soft clay caused by long-term cyclic loads subjected to traffic loads. Mar Georesour Geotechnol 39(4):398–407
36. Wichtmann T, Triantafyllidis T (2018) Monotonic and cyclic tests on kaolin: a database for the development, calibration and verification of constitutive models for cohesive soils with focus to cyclic loading. Acta Geotech 13:1103–1128
37. Xiao J, Juang CH, Wei K, Xu S (2014) Effects of principal stress rotation on the cumulative deformation of normally consolidated soft clay under subway traffic loading. J Geotech Geoenviron Eng 140:04013046
38. Xiao J, Zhang D, Wei K, Luo Z (2017) Shakedown behaviors of railway ballast under cyclic loading. Constr Build Mater 155:1206–1214
39. Xu Z, Pan L, Gu C, Cai JY (2020) Deformation behavior of anisotropically overconsolidated clay under one-way cyclic loading. Soil Dyn Earthq Eng 129:105943
40. Zhang D, Xiao J, Zhang X (2018) Effects of pier deformation on train operations within high-speed railway ballastless track-bridge systems. Transport Res Rec 036119811877652